Journal Pre-proof

Effects of dynamic land use/land cover change on water resources and sediment yield in the Anzali wetland catchment, Gilan, Iran

Helen Aghsaei, Naghmeh Mobarghei Dinan, Ali Moridi, Zahra Asadolahi, Majid Delavar, Nicola Fohrer, Paul Daniel Wagner

PII: S0048-9697(19)36445-9

DOI: https://doi.org/10.1016/j.scitotenv.2019.136449

Reference: STOTEN 136449

To appear in: *Science of the Total Environment*

Received date: 17 October 2019

Revised date: 30 December 2019

Accepted date: 30 December 2019

Please cite this article as: H. Aghsaei, N.M. Dinan, A. Moridi, et al., Effects of dynamic land use/land cover change on water resources and sediment yield in the Anzali wetland catchment, Gilan, Iran, *Science of the Total Environment* (2020), https://doi.org/10.1016/j.scitotenv.2019.136449

Effects of dynamic land use/land cover change on water resources and sediment yield in the Anzali wetland catchment, Gilan, Iran

Helen Aghsaei [a, b, *], Naghmeh Mobarghei Dinan [a], Ali Moridi [c], Zahra Asadolahi [d], Majid Delavar [e], Nicola Fohrer [b], Paul Daniel Wagner [b]

[a] Environmental Sciences Research Institute, Shahid Beheshti University, 1983969411 Tehran, Iran

[b] Department of Hydrology and Water Resources Management, Institute for Natural Resource Conservation, Kiel University, D-24118 Kiel, Germany

[c] Abbaspour College of Technology, Shahid Beheshti University, 16589-53571 Tehran, Iran

[d] Department of Agriculture and Natural Sciences, Lorestan University, 68151-44316 Lorestan, Iran

[e] Department of Water Resources Engineering, Tarbiat Modares University, 14115-111 Tehran, Iran

Effects of dynamic land use/land cover change on water resources and sediment yield in the Anzali wetland catchment, Gilan, Iran

Abstract

Land use/land cover (LULC) changes strongly affect catchment hydrology and sediment yields. The current study aims at analyzing the hydrological consequences of dynamic LULC changes in the Anzali wetland catchment, Iran. The Soil and Water Assessment Tool (SWAT 2012) model was used to assess impacts on evapotranspiration, water yield, and sediment yield. Two model runs were performed using static and dynamic LULC inputs to evaluate the effects of LULC change between 1990 and 2013. For the static model, the LULC map of 1990 was used, whereas for the dynamic model, a gradual change of the LULC distribution was interpolated from 1990, 2000, and 2013 LULC data. The major LULC changes were identified as an increase of agricultural area by 7% of the catchment area and a decrease of forest coverage by 6.8% between 1990 and 2013. At the catchment scale, the differences in the long-term mean annual values for the main water balance components and sediment yield were smaller than 10 mm (<2.8%) and 3 t/km^2 (<2.6%), respectively. However, at the sub-basin scale the increase of agricultural land use resulted in an increase of evapotranspiration, water yield, and sediment yield by up to 8.3%, 7%, and 169%, respectively, whereas urban expansion led to a decrease of evapotranspiration, water yield, and sediment yield by up to -3.5%, -2.3%, and -9.4%. According to the results of the monthly time scale analysis, the most significant impact of LULC changes occurs during the dry season months, when the increase of irrigation agriculture results in an increase in water discharge and sediment loads to the Anzali wetland. Overall, the results showed that the

implementation of dynamic LULC change into the SWAT model could be adopted as a planning tool to manage LULC change of the Anzali wetland catchment in the future.

Keywords: SWAT model, Dynamic LULC, Water balance, Sediment yield

1. Introduction

Current global trends, such as population and economic growth which often lead to increased food and fuel demands, exert increasing pressure on land and water resources worldwide (Grey et al., 2014; Biswas et al., 2002). Additionally, land use/land cover (LULC) changes have potentially large impacts on hydrologic processes (Anand et al., 2018; Stonestrom et al., 2009). These may include changes in total suspended sediment and nutrient concentration (Hwang et al., 2016), flood frequency, baseflow, annual mean discharge (Rogger et al., 2017; Li et al., 2018; Nie et al., 2011), seasonal variation in streamflow (Guo et al., 2008), evapotranspiration (Pinto Dias et al., 2015; Wang et al., 2012), surface runoff generation (Shi et al., 2007), soil water content (Zhang and Shangguan, 2016), and groundwater recharge (Mishra and Kumar, 2015). The major factors contributing to LULC change include rapid socio-economic development, national resource conservation policies, and climatic variability (Dwarakish and Ganasri, 2015; Elfert and Bormann, 2010; Mao and Cherkauer, 2009). Particularly in regions where water availability is limited, LULC changes could result not only in the deterioration in water quality, but also in an increase of water scarcity. Therefore, an assessment of the impacts of anthropogenic LULC alteration on hydrology is crucial for sustainable river basin management (Ahiablame and Shakya, 2016).

To assess impacts of LULC change on the hydrologic response of a catchment, LULC information derived from RS data has been used in various hydrologic models, e.g., Hydrological Simulation Program-Fortran (HSPF) model (Jing and Ross, 2015), SWAT (Bieger et al., 2015) MIKE SHE (Im et al., 2009), HEC-HMS (Zubair Younis and Ammar, 2018), PRMS (Legesse et al., 2010), HBV (Ashagrie et al., 2006), DHSVM (Safeeq and Fares, 2012), and WaSiM-ETH (Bormann and Elfert, 2010).

Through comparison of hydrological models for evaluating the effect of different land management practices, distributed hydrological models are efficient tools as they could account for spatial heterogeneity and, consequently, they have a higher accuracy for predicting the effect of LULC on hydrological processes (Cornelissen et al., 2013; Dwarakish and Ganasri, 2015). Among these models, SWAT has been widely applied around the world to assess impacts of LULC change on catchment hydrology. For example, Ghaffari et al. (2010) employed SWAT to determine the effect of LULC change on the hydrological response of the Zanjanrood catchment, Iran. The results showed an increase in runoff and a decrease in the groundwater recharge due to a replacement of grasslands with rain-fed agriculture and bare soil. Zhu and Lie (2014) applied it to examine the hydrological impacts of LULC change in the Little River catchment in the Unites States using a detailed LULC record from 1984 to 2010. They showed that a 3% increase in streamflow was closely related to urban expansion, whereas a reduction of 34.6% in sediment and of about 10% in nutrient loads was mostly related to the decrease of agricultural land. Lotz et al. (2018) used SWAT to quantify the hydrological response of Dongting Lake basin in China to LULC change (2000 and 2013). They reported that the conversion of agricultural land into forest decreased surface runoff and total water yield, while it increased evapotranspiration, interflow, and ground water flow.

However, most SWAT model applications assessed the hydrological impacts based on static LULC data (Teklay et al., 2019), in which the comparison of model runs for a given time period is based on different LULC maps. This approach does not account for potentially non-linear impacts of LULC changes (Wagner et al., 2016, 2019), which could affect the hydrological responses of a catchment. Hydrological modeling by implementing a single LULC layer could introduce a source of additional uncertainty (Pai and Saraswat, 2011) as it cannot represent a realistic development within the modeling period. Whereas, by simulating dynamic land-use change patterns throughout the hydrologic simulation period, the long-term effects of human–environment interaction can be assessed more accurately. For example, Lamparter et al. (2016) integrated an annual land use update model with SWAT for the hydrological modeling of two macro-catchments in Southern Amazonia, Brazil. They concluded that dynamic representation of land use changes in the SWAT model could improve the model performance especially in regions with intensive land use change. Similarly, Teklay et al. (2019) implemented both static and dynamic LULC changes in the SWAT model to investigate the effects of dynamic LULC on hydrological responses of the Gummara catchment, Ethiopia. They declare that implementing dynamic LULC data has improved representation of the dynamic catchment characteristics.

The Anzali wetland catchment in Iran contains ecologically significant ecosystems such as the Anzali wetland and the Hyrcanian forests. It is also one of the important rice-growing regions of Iran. In recent decades the catchment has been subjected to environmental issues like urban sprawl and gradual land degradation (Jafari et al., 2016) that potentially have negative impacts on various hydrological components in the catchment. Some studies have been carried out in the Anzali wetland catchment. For example, Zamani Hargalani et al. (2014) introduced a new pollution index to measure the total concentration of metals in the sediments of the Anzali

wetland. Likewise, Ghafouri et al. (2010) simulated the pollution loads in one of the sub-catchments of the Anzali wetland. Nevertheless, no study has so far considered the hydrological effects of LULC change in the Anzali wetland catchment. Thus, the aim of this study is to analyze the spatio-temporal impacts of long-term LULC change on the water balance components and sediment yield of the Anzali wetland catchment.

2. Materials and methods

2.1. Study area

The catchment of the Anzali wetland is located in the Gilan province of Iran on the southern coast of the Caspian Sea (36° 54'-37° 28' N, 48° 48'- 49° 37' E; fig. 1), which drains an area of approximately 3344 km² into the Anzali wetland. The elevation of the catchment ranges from -25 m below mean sea level to 3073 m above mean sea level. The regional climate is classified as a Caspian-Hyrcanian climate with an average temperature of 8°C in the coldest month and 23°C in the warmest month. The long-term mean annual rainfall is 1300 mm with significant spatio-temporal variability, 40% of which is confined to the autumn season (September to January), so that the precipitation amount is lower than the crop water requirement in spring and summer.

The Anzali wetland catchment is composed of two types of landforms; a lowland area in the north-east and a mountainous area in the south-west. The land use of the catchment is dominated by agricultural land with fertile and productive soil types at lower elevations. About 70% of the agricultural area is under rice plantation and the remaining is mostly rain-fed agriculture. Hyrcanian forests are mostly at higher elevations and grassland can be found on the western and southern borders of the catchment. Urban area is scattered mainly from the east where the capital

city of the state, Rasht, is located, to the center of the catchment in proximity to areas that are suitable for agriculture. Water for irrigation agriculture is mainly provided by surface water. Approximately 80% of the irrigation water is transferred to the catchment from the Sefidrood river through two diversion dams which transfer water to two main irrigation canals (Fig. 1).

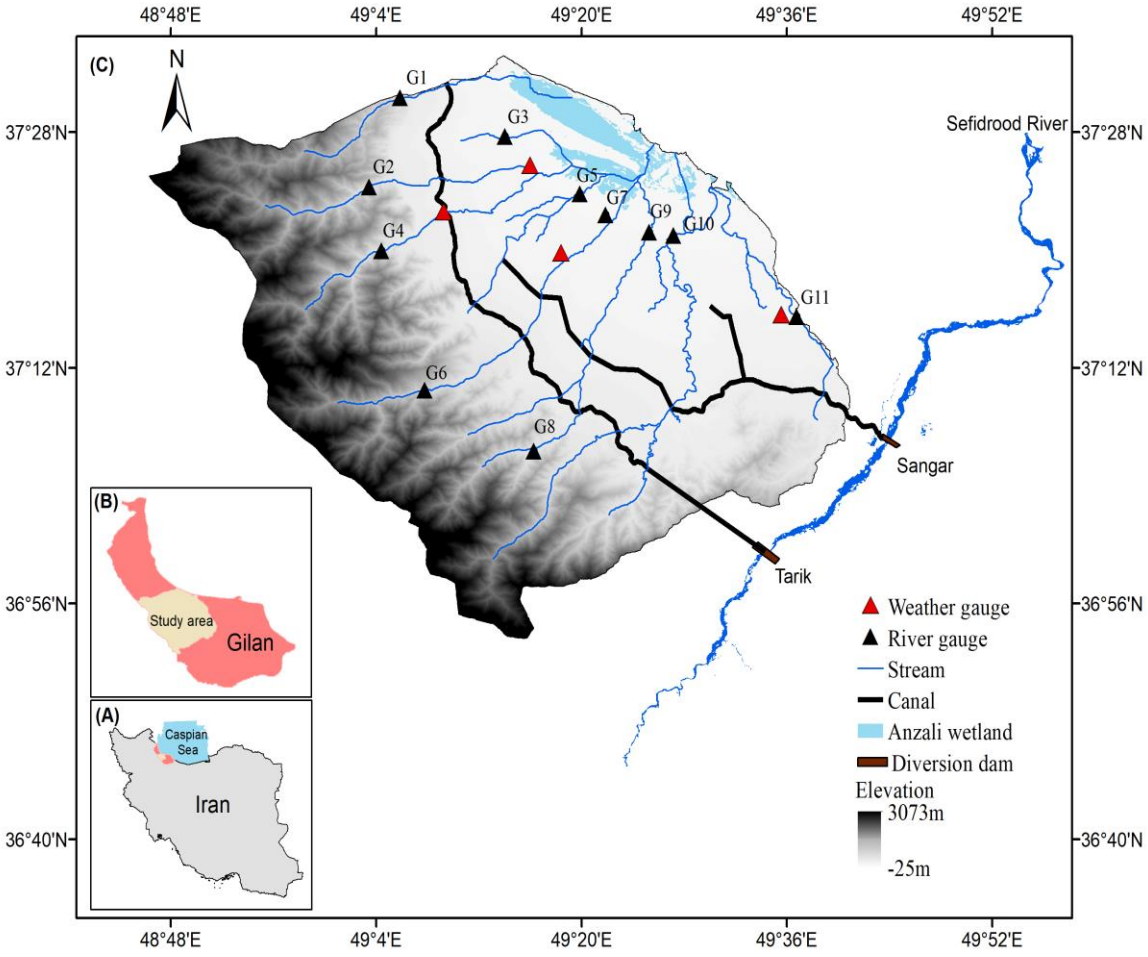

Fig. 1. The Anzali wetland catchment in the Gilan province (B) of Iran (A) depicted with streams, river gauges, weather gauges, irrigation canals, and diversion dams (C).

2.2. LULC classification

LULC classifications for 1990, 2000, and 2013 were derived from satellite data. Landsat 5 Thematic Mapper (TM) images acquired in May 1990 and May 2000 and Landsat 7 Enhanced Thematic Mapper Plus (ETM+) satellite imagery acquired in May 2013 were used (USGS 1990, 2000, and 2013). These images were selected as they are cloud-free and they are representative of the cropping season of the catchment, so that agricultural land is accurately identified (Wilken et al., 2017).

To process the satellite data and quantitatively assess LULC change in the study area, ArcGIS and ERDAS Imagine software were used. All the images were resampled to 30 m * 30 m pixel resolution using nearest neighbor resampling to preserve the original image radiometry (Burns and Nolin, 2014). The images were geo-referenced and geocoded to Universal Transverse Mercator (UTM) Zone 39 N and radiometric and atmospheric correction were carried out. Ground truth (200 points) from a field survey and from a land use map of the Plan and Budget Organization of Iran (PBO, 2013) was used for supervised LULC classification and accuracy assessment of the classification results. The Crosta method was used for False Color Composite (FCC) creation of training areas (Crosta and Moore, 2007), and a classification was carried out using a maximum likelihood algorithm. Six major LULC classes were extracted and classified: forest, agriculture land, grassland, wetland, water, and urban areas. The accuracy of the classification was assessed for the three supervised classifications based on the ground truth. The overall classification accuracy was 91% for 1990, 88.2% for 2000, and 85.8% for 2013. The Kappa coefficients of 0.90, 0.87, and 0.85 denote an almost perfect inter-rater agreement for the classified maps of 1990, 2000 and 2013, respectively (Yang and Lo, 2002).

2.3. Hydrologic modeling

In this study, the GIS interface ArcSWAT-2012 was used to set up a SWAT model of the Anzali wetland catchment. The SWAT model (Arnold et al., 1998) requires input data for topography, soil, and land use along with hydro-meteorological data to simulate hydrological processes. Model calculations are based on hydrologic response units (HRUs) representing lumped areas with a unique land use, soil, and slope class combination within a sub-basin. The following data inputs are used to set up the SWAT model: a Digital Elevation Model (DEM) with a spatial resolution of 30 m was derived from ASTER satellite data (GDEM V_2), soil spatial distribution data and soil parameters were obtained from the global soil map of the Food and Agriculture Organization (FAO, 1995), and LULC maps for the years 1990, 2000, and 2013 were prepared as presented in detail in section 2.2. As mentioned before, rice is cultivated with irrigation in 70% of the agricultural land use of the catchment, and the remaining cultivation is rain-fed agriculture with diverse orchard crops that are highly variable in space. Because of the coarse resolution of the available RS LULC data, it was not possible to distinguish between these crop types precisely (Yan et al., 2013). Therefore, the agricultural land use class was split into rice (70%) and orchard (30%) using the land use refinement tool in SWAT, except for those agricultural areas located in the upstream part of the catchment, which were defined as orchards since no rice is cultivated in this area.

Management operations for rice and orchards as derived from field work and expert knowledge were set up in the SWAT model (Table 1). Irrigation water for rice fields was extracted from the river reach or was taken from a source outside of the catchment, as irrigation water is transferred to the catchment with irrigation canals (Fig.1).

Table 1. Agriculture operation information

SWAT operations	Operation time/(per year) for rice	Operation time/(per year) for Orchard
Plant/begin growing season	1 April	15 September
Irrigation	From 2 April to 10 September	-
First fertilization	20 April (urea,220 kg/ha)	1 October (phosphate ,200 kg/ha)
Second fertilization	22 April (phosphate,100 kg/ha)	2 October (urea,300 kg/ha)
Harvest (and kill)	15 September	10 November

Weather data for the period from 1990 to 2013 were used. Daily rainfall, minimum/maximum temperature, solar radiation, wind speed, and average humidity data were collected from four Iran Meteorological Organization stations within the study area. Because the spatial density of the precipitation stations is very low in the Anzali wetland catchment and all four precipitation stations are located at elevations below 35 m, changes of precipitation with elevation are not well represented in the upstream part of the catchment. Therefore, ten elevation bands were defined in each sub-basin following Fontaine et al. (2002). Further, precipitation lapse rate (PLAPS) and temperature lapse rate (TLAPS) were used to adjust precipitation and temperature for elevation bands. Since PLAPS and TLAPS are driving variables and affect almost all other model parameters, 200 simulations were performed for these two parameters to determine their values based on the best simulation result. Finally, a precipitation lapse rate of 220 mm and a temperature lapse rate of 6°C per 1 km were specified.

As daily streamflow data were not available for all of the hydrological stations, monthly streamflow data from eleven hydrological stations were used. This data covers both landforms in the catchment, i.e. the lowland areas and the mountain areas (Fig. 1). Sediment concentration data was also available for 10 hydrological stations. The streamflow and sediment data were

obtained from the Iran Water Resources Management Company. This data was available from 1990 to 2013.

The surface runoff was calculated using the SCS curve number approach (SCS, 1972) and the Penman–Monteith equation was used to calculate the potential evapotranspiration (Allen et al., 1989). This approach is used in various SWAT modeling studies in regions containing irrigated paddy fields (e.g., Liang et al., 2016; Sakaguchi et al., 2014).

To study the hydrological impacts of LULC change in the Anzali wetland catchment, two different model runs were set up: a static model run using the LULC of 1990 and a dynamic model run using land use updates. For this purpose, the Land Use Update tool (LUU) (Pai and Saraswat, 2011) was used to obtain the HRU- fractions for 1990, 2000, and 2013 land use maps. Then, HRU-fractions for each year of the simulation period were calculated using a linear interpolation of annual land use change from 1990 to 2000 and 2000 to 2013.

The Anzali wetland catchment consists of nine main streams that drain into the Anzali wetland. We used two SWAT models, one for the northern and another one for the southern streams, to model the entire catchment, which allows us to better represent the entire catchment. Based on the DEM, land use, and soil data, the Anzali wetland catchment was divided into 30/34 sub-basins and 822/1004 HRUs in the two delineated sub-catchments. The entire Anzali wetland catchment consists of 64 sub-basins and 1826 HRUs.

After the setup and delineation of the static LULC model in ArcSWAT, a sensitivity analysis was performed in SWAT-CUP (Abbaspour et al., 2007) based on the sequential calibration method. According to this method, once satisfactory calibration performance was obtained for streamflow, sensitivity analysis was carried out for the sediment parameters. The sensitivity analysis of streamflow and sediment related model parameters was achieved by performing a

local (one-at-a-time) sensitivity analysis (Shope et al., 2014). Then, intensive manual calibration for streamflow was performed at the eleven monitoring stations in order to reduce the acceptable parameter ranges at each site. The optimized parameter ranges were incorporated into the SUFI-2 auto-calibration routine (Abbaspour et al., 2007). The static model setup was calibrated for streamflow from 1990 to 2000 using a 3 years model spin-up phase. Sediment calibration and validation were performed at the ten gauging stations for the same period as streamflow. To estimate sediment yield, the Modified Universal Soil Loss Equation (MUSLE) is used in the SWAT model (Williams, 1975). We applied a multi-site calibration by calibrating the upstream gauges first and keeping the calibrated parameters constant for the upper catchment when calibrating the downstream gauge afterwards. Model performance was evaluated by comparing modeled and observed monthly discharge data. Streamflow was validated for the period from 2001 to 2013. The model performance in simulating streamflow and sediment yield was then evaluated using percent bias (PBIAS) and Nash–Sutcliffe coefficient of efficiency (NSE, Nash and Sutcliffe, 1970).

For the SWAT model with dynamic LULC updates, we used the same parameters as derived from the calibration of the static model. To assess the impacts of LULC changes, we compared the results from the dynamic model to the static baseline model. With this modeling approach hydrologic response is isolated to a single variable (LULC change), so that the differences in the static and dynamic model outputs is a result of LULC change. The same method was used in similar studies (e.g., Koch et al., 2012, Wagner et al., 2016, 2019). We focus on the effects of dynamic LULC change on evapotranspiration (ET), water yield (WYLD), and sediment yield (SYLD) on the catchment and sub-basin scale. In SWAT, WYLD is defined as the net amount of water that leaves the sub-basin and contributes to streamflow. WYLD is the sum of surface

runoff (SURQ), interflow (LATQ), and baseflow (GWQ), subtracting transmission losses (TLOSS) and pond abstractions (POND) (Neitsch et al., 2010).

3. Results and discussion

3.1. LULC change analysis

In the year 1990, the upper part of the Anzali wetland catchment is dominated by forest (45.8%), followed by agricultural land (40.8%) in the middle and lower part. Grassland covers 8% and is mostly found at the border of the forest coverage. Wetland, water, and urban areas accounted for 2.5%, 1.4%, and 1.5% of the catchment in 1990. The spatial distribution of the major LULC classes in 1990, 2000, and 2013 is shown in the supplementary document.

Comparing the LULC data of the years 1990, 2000, and 2013, the most obvious LULC changes occurred in the agricultural and forest land use classes (Table 2). From 1990 to 2013, the areal coverage of agricultural land use increased by 7% of the catchment area (234 km^2), which is an average increase of about 10 km^2 per year. As Table 3 shows, agricultural land mainly increased at the cost of forest coverage: 76% of the area converted to agriculture was forest in 1990 (177.8km^2), 12.5% was grassland (29.3 km^2), and 11.4% was wetland (26.7 km^2). Forest, grassland and wetland showed a decline by -6.8% (227.4 km^2), -1.0% (33.4 km^2), and -0.7% of the catchment area (23.4 km^2), respectively. Most of the lost forest area was converted to agriculture (91%) and about 9% was converted to grassland. The lost wetland was entirely (100% of the area) converted for agricultural purposes. The water area of the catchment is assumed to remain constant during the study period.

Urban area changed the most in relative terms among all the LULC classes, increasing to 100% in 2013 as compared to 1990. However, the expansion of the urban class is not substantial with respect to the total area of the catchment, i.e., an increase of 1.5% (50.2 km^2). According to

Table 3, the increase in urban land use was at the expense of agricultural area (93.1%) and mainly occurred around the cities of Somesara, Rasht, and Fuman due to significant population growth in the years between 1990 and 2013 by 38%, 25%, and 11%, respectively (Akbari et al., 2015). Changes from urban area to agriculture are unlikely and may have resulted from a misclassification of urban area in 1990 or a misclassified agriculture in 2013. However, these changes comprise only 0.1% of the 8.9% of the catchment area that was changed to agriculture and, therefore, indicate a small, acceptable uncertainty of the approach. In addition, the observed changes from agriculture and grassland to forest (0.1% of the catchment area) may be due to the misclassification since no reforestation has been observed in the catchment during the study period. Comparing the two sub-periods (1990–2000 and 2000–2013), the LULC changes follow a similar trend in both sub-periods. However, there is a larger increase of agricultural area and decrease of forest coverage during the second sub-period (+137.1/-147.1 km^2) than during the first sub-period (+97.0/-80.3 km^2). Hence, the decrease rate of forest almost doubled in the second sub-period, showing that the deforestation rate has accelerated after the year 2000.

Table 2. Land use/land cover (LULC) area percentage and changes for 1990-2013 in the Anzali wetland catchment

LULC	Fraction			Change (%)
	1990	2000	2013	(1990-2013)
Wetland	2.5%	2.2%	1.8%	-0.7%
Agriculture	40.8%	43.7%	47.8%	7.0%
Forest	45.8%	43.4%	39.0%	-6.8 %
Grassland	8.0%	7.2%	7.0%	-1.0%
Residential area	1.5%	2.1%	3.0%	1.5%
Water	1.4%	1.4%	1.4%	0.0%
Total	100%	100%	100%	

Table 3. Information on the changed land use/land cover (LULC) in the catchment (11.6% of the catchment area): (i) distribution of 1990 LULC classes of areas converted into the 2013 LULC. (ii) Area changed into the 2013 LULC as percentage of the catchment area.

		Land use/land cover in 2013					
		Agriculture	Forest	Grassland	Urban	Wetland	Water
(i) Land use/land cover in 1990	Agriculture	0.0%	0.2%	25%	93.1%	0.2%	0.0%
	Forest	76.0%	0.0%	75%	2.1%	0.0%	0.0%
	Grassland	12.5%	98.8%	0.0%	4.8%	98.8%	0.0%
	Urban	0.10%	0.0%	0.0%	0.0%	0.0%	0.0%
	Wetland	11.4%	0.0%	0.0%	0.0%	0.0%	0.0%
	Water	0.0%	0.0%	0.0%	0.0%	0.0%	0.0%
(ii) Changed area with 2013 land use/land cover as percentage of the catchment area		8.9%	0.1%	0.9%	1.5%	0.2%	0.0%

3.2. Calibration and validation of the SWAT model

For the streamflow calibration in SWAT-CUP, eighteen parameters were initially selected and, finally, ten parameters with the highest sensitivity values were selected to be adjusted for each monitoring station through the discharge calibration process (Supplementary material, Table A1). The set of calibrated SWAT model parameters and their adjusted values at each gauging station are shown in Table 4. The surface runoff response parameters are SCS CN II value (CN2), the soil evaporation compensation factor (ESCO), available water capacity of the soil layer (SOL_AWC), saturated hydraulic conductivity of the soil layer (SOL_K), and subsurface response parameters include ground water delay (GW_DELAY), the threshold water depth in the shallow aquifer for flow (GWQMN), deep aquifer percolation fraction (RCHRG_DP), deep aquifer percolation fraction (RCHRG_DP), and plant uptake compensation factor (EPCO). A basin response parameter, effective hydraulic conductivity in main channel alluvium (CH_K2), was also used for the streamflow calibration. Among the parameters, CN2 was found to be the most sensitive parameter at all stations (See supplementary material, Table A1), which is in agreement with several other studies (e.g., Wang et al., 2012; Zhao et al., 2016; Briak et al., 2016). The final value of parameters for streamflow calibration at each gauging station are given in Table 4. For CN2, SOL_AWC and SOL_K percentage-based variations were used to maintain their spatial variability. The curve number is highly related to the land use type. For the downstream stations (G5, G7, G9, G10) the curve number was increased. These areas have a large percentage irrigation agriculture. Higher CN2 values result in higher runoff and less infiltration (Teklay et al., 2019). On the contrary, CN2 values were decreased for upstream stations (G1, G2, G4, G6, G8) that are characterized by mountainous areas and forest, allowing for a slower runoff response. Higher values of CN2 as well as lower values of GWQMN,

RCHRG_DP, and SOL_AWC for downstream stations indicate a quicker response towards surface runoff generation.

As sediment yield is a function of runoff processes, strong overlapping patterns between sediment yield and runoff was observed. However, the initial SWAT run showed a significant overestimation of the sediment at all stations. Therefore, to decrease simulated sediment yields, a sensitivity analysis was carried out with twelve sediment-related parameters at each station. In the end, four parameters with the highest sensitivity values (Supplementary material, Table A1) were used for the sediment calibration. Among the parameters, the peak rate adjustment factor for sediment routing in the sub-basin (ADJ_PKR) was the most sensitive, followed by the USLE support practice factor (USLE_P), sediment concentration in lateral flow and groundwater flow (LAT_SED), and the USLE soil erodibility factor (USLE_K). ADJ_PKR adjusts the effect of peak flow rate on sediment routing in tributary channels and have a major impact on sediment transportation (Dakhlalla and Parajuli, 2019). USLE_P is important to control the high simulated erosion rates (Bieger et al., 2012). Higher values of USLE_P and USLE_K were assigned for the downstream stations (G5, G7, G9, G10), which indicates that there is a high soil loss in the agricultural areas. LAT_SED values have been increased at all stations, which means the sediment concentration in lateral flow and groundwater flow contribute to total sediment yield of the catchment due to the high amount of return flow.

The NSE and PBIAS values for the monthly calibration and validation of streamflow and sediment yield at the gauging stations are shown in Table 5. The NSE coefficient for the calibration of streamflow and sediment yield ranges from 0.55 to 0.75 and 0.50 to 0.70, and the PBIAS values ranges from -12.57 to 10.97 and 0.28 to 14.09, respectively. For the validation period, the NSE coefficient ranges from 0.41 to 0.69 for streamflow and from 0.50 to 0.68 for the

sediment yield, and the PBIAS values ranges from -17.80 to 10.56 and -18.64 to 2.92 for streamflow and sediment yield, respectively. These results suggest satisfactory to good model performance (Moriasi et al., 2007). Only station G4, has an NSE below 0.50 in the validation period of streamflow (calibration: 0.72), as peak flows were underestimated, whereas the general water balance is well represented (PBIAS = -0.02). According to Bieger et al. (2012) and Lotz et al. (2018) localized precipitation events occurring in remote parts of a catchment cannot be captured by the meteorological stations, so that the precipitation adjustment with the help of elevation bands is not successful in this sub-basin.

Table 4. The values of parameters used for the calibration of streamflow and sediment yield at each gauging station

Parameters used	Final parameter value										
to calibrate streamflow	G1	G2	G3	G4	G5	G6	G7	G8	G9	G10	G11
r__CN2	-45%	-47%	-8%	-40%	+10%	-43%	+21%	-38%	+10 %	+20%	+2.5%
v__ESCO	0.95	0.94	0.98	0.92	0..80	0.75	0.89	0.84	0.90	0.87	0.91
v__EPCO	0.55	0.96	0.91	0.93	0.75	0.91	0.95	0.99	0.97	0.99	0.95
v_GW_DELAY	18.5	21	24	21	30	35	37	35	47	36	34
v__GWQMN	800	585	480	650	349	850	420	650	175	420	422
v__RCHRG_DP	0.77	0.6	0.54	0.7	0.18	0.55	0.42	0.53	0.45	0.46	0.42
v__GW_REVAP	0.02	0.02	0.03	0.02	0.03	0.02	0.03	0.03	0.03	0.01	0.02
r__SOL_K	+26%	+47	+31%	+40%	+44%	+48%	+42%	+43%	+47%	+40%	+40%
r__SOL_AWC	+34%	+30%	+12%	+35%	+21%	+46%	+17%	+36%	+22%	+26%	+21%
v__CH_K2	30	48	30	30	31	30	30	30	28	25	38
Parameters used to	Final parameters value										
calibrate sediment yield	G1	G2	G3	G4	G5	G6	G7	G8	G9	G10	G11
v__ADJ_PKR	0.49	0.49	0.49	0.49	0.49	0.49	0.49	0.49		0.45	0.49
v__USLE_P	0.09	0.02	0.09	0.05	0.23	0.01	0.13	0.04		0.15	0.17
v__USLE_K	0.21	0.22	0.22	0.14	0.33	0.15	0.47	0.05		0.32	0.21
v__LAT_SED	46.6	42.2	45	45.3	62	42	55.5	41.4		45.5	42.2

Table 5. Statistical analysis results for calibration and validation periods

Monitoring station	NSE		PBIAS	
	Streamflow	Sediment yield	Streamflow	Sediment yield
Calibration period (1990-2000)				
G1	0.65	0.59	5.61	1.51
G2	0.67	0.55	4.50	6.15
G3	0.57	0.59	10.97	0.28
G4	0.72	0.66	-0.02	2.47
G5	0.71	0.50	3.40	9.43
G6	0.55	0.53	8.21	5.23
G7	0.62	0.58	-12.57	6.10
G8	0.60	0.58	3.21	6.84
G9	0.58		2.37	
G10	0.75	0.70	-2.70	7.75
G11	0.71	0.59	1.10	14.09
Validation period (2001-2013)				
G1	0.55	0.53	2.53	-18.64
G2	0.61	0.53	0.31	-5.00
G3	0.66	0.68	-2.51	0.05
G4	0.41	0.50	10.56	-3.23
G5	0.68	0.59	-2.30	-4.31
G6	0.58	0.50	-0.92	-14.42
G7	0.63	0.51	-17.80	-5.35
G8	0.58	0.54	-11.90	2.92
G9	0.56		-13.21	
G10	0.65	0.57	-14.69	-13.07
G11	0.69	0.54	-2.23	-15.94

3.3. Assessment of hydrological response to dynamic land use change

3.3.1 Hydrological response at the catchment scale

The results of a model run with static land use and a model run with dynamic land use were used to analyze the spatio-temporal effects of dynamic LULC change on water resources and sediment yield in the catchment. The mean annual basin values for the different water balance components simulated by static and dynamic land use data are shown in Table 6. The results show that water yield has a slightly higher proportion of precipitation than evapotranspiration. The difference in the hydrological response between the two applied models provide the isolated impact of land use change. The differences in the long-term average annual values for water balance components are smaller than 10 mm on the catchment scale. The estimated ET, WYLD, and SURQ in the dynamic land use model increased by 0.9%, 1%, and 2.8%, respectively. Total sediment loading is also increased by 2.6% (3 t/km^2) through the dynamic land use model. A possible reason for the increase in ET is the conversion of forest to irrigated paddy fields. Also, a positive impact on SURQ and WYLD can be observed as almost 80% of the irrigation water for the expanded rice fields are taken from outside the catchment (Sefidrood river). The slight decrease in groundwater flow and lateral flow can be attributed to less soil infiltration and more surface runoff (Ayivi and Jha, 2018).

It is a commonly known effect that impacts of LULC change are small when aggregated in space and time (Fohrer et al., 2001; Wagner et al., 2013). Other studies that considered dynamic land use change in hydrologic modeling also report relatively small impacts on the annual water balance components. In a meso-scale catchment in India, Wagner et al. (2016) did not identify significant effects on the hydrological response on the catchment scale. Chu et al. (2010) conclude that even though dynamic land use change modeling is more realistic than using static

land use change, it has only a slight influence on the variability and magnitude of the streamflow in the studied area (Wu-Tu catchment in Taiwan). Likewise, Wang et al. (2018) points out that the monthly hydrological response was more affected by the dynamic land use implementation than annual response.

Table 6. Average annual water balance components and sediment yield for the entire catchment. Revap is the amount of water moving from shallow aquifer to plants/soil profile in the catchment

Variable	Static land use	Dynamic land use
Precipitation (mm)	1164	1164
Irrigation (mm)	136.75	143.65
Revap (mm)	14.75	14.75
Evapotranspiration (mm)	606.31	611.85
Total water yield (mm)	720.28	727.83
Surface runoff (mm)	334.08	343.30
Groundwater flow (mm)	254.46	254.11
Lateral flow (mm)	131.74	130.42
Sediment yield (t/ha)	1.17	1.20

3.3.2. Hydrological response at the sub-basin scale

The effect of dynamic land use change on the hydrological response was more discernible on the sub-basin scale. To relate the magnitude and direction of these changes to the changes in land use data, spatial distribution of the main land use changes at sub-basin level between 1990 and 2013 were assessed (Fig. 2). During this period, the agricultural land use area increased mainly in the midstream sub-basins with a maximum expansion of 31.3% in sub-basin 41. Urban sprawl occurred in the mid-eastern part of the catchment with the greatest increase (>12%) in sub-basins

23, 25, 8, and 26, respectively. In the northern sub-basins directed toward the catchment outlet, up to 16.6% of the sub-basin area changed from wetland to agriculture. The expansion of agricultural land and urban area account for almost 80% of the total land use changes of the catchment from 1990 to 2013.

Fig. 3 (A) shows the percentage change of long-term ET per sub-basin. The changes in long-term mean annual ET range from a decrease of −3.5% (−24 mm/year) in one small sub-basin (23) to an increase of 8.3% (54.9 mm/year) in sub-basin 6. In the middle stretches in the eastern part of the catchment, the decrease in ET spatially corresponded to sub-basins in which the major land use change is from agriculture to urban. Likewise, the maximum expansion of urban land use by 36.5% can explain the decrease of ET in sub-basin 23. This is in agreement with the reduction of ET and surface runoff increase due to the expansion of urban land use reported in other studies (Anand and Khosa, 2018; Aladejana et al., 2018)

Due to the expansion of irrigated agriculture (rice fields) in most of the sub-basins, ET is increased in almost 80% of the catchment area. The increase of ET can be attributed to the intensive irrigation of the rice fields during the dry season. Between April and September, water withdrawal from the rivers and water transfer from outside the catchment for irrigation activities can be observed in sub-basins with an increase of rice fields. Whereas for the sub-basins with the increased dry farming (orchards), which are mainly located in the uppermost portions of the catchment, no perceptible change in average annual ET (<1%) was observed. These findings are in agreement with the work by Schmidt et al. (2009), who claimed that average annual ET could increase significantly under intensified irrigation scenarios, when compared to dryland farming In sub-basin 26, there is an almost similar expansion of both urban and agricultural land use

(12%), so that the opposing effects of land use change on ET balance each other (ET change = 0.46%).

Sub-basin level change of WYLD using the long-term average of static and dynamic land use simulation is shown in Fig. 3(B). Changes in mean annual WYLD range from a decrease of -2.3% (15.2 mm/year) in sub-basin 23 to an increase of 6.9% (56.7 mm/year) in sub-basin 41. Sub-basins with a substantially increased mean annual WYLD are those sub-basins which also showed more pronounced increased ET, indicating the significant influence of irrigated agricultural expansion on the main water balance components of the catchment. Consequently, the highest agricultural land use expansion (31.3%) caused the highest WYLD variation in sub-basin 41. Wagner et al. (2013) showed similar findings in the Mula and Mutha Rivers catchment, India, where the expansion of irrigated cropland areas increased ET and WYLD at the same time as more water was available due to irrigation.

A major decrease of mean annual WYLD occurred in sub-basins 23 and 8 where the main land use change is urban expansion at the expense of agriculture area. Only slight decreases of WYLD were detected in the upstream part of the catchment. As the expansion of built-up area resulted in increased surface runoff due to decreased water infiltration, the fraction of the water yield contribution from base flow has significantly decreased so that the overall effect on water yield was a reduction by -2.3% and -1% in sub-basins 23 and 8, respectively. According to Douglas (1983), the increase of the surface runoff and decrease in groundwater flow is due to an increased impermeability and ground sealing effect.

The impacts of dynamic land-use change on mean annual sediment yield at sub-basin level is shown in Fig. 3(C). Changes in SYLD ranges from a decrease of -9.43% (-6 t/km^2/year) in sub-basin 23 to an increase of 169.4% (76 t/km^2/year) in sub-basin 41. The main factor associated

with the highest sedimentation rates (e.g., at sub-basins 41, 50, 51, and 60) is the increased WYLD as a result of substitution of forest areas with irrigated agriculture. Whereas urban expansion decreased sedimentation due to the decreased WYLD, so that in sub-basins 23 and 8 the maximum expansion of urban land use by 36.5% and 13% can explain the decrease of SYLD by -9.43% and -9.1%, respectively. For the sub-basins with the increased non-irrigated orchards, no discernible changes were observed. Similar results about high rate of soil loss due to the expansion of irrigated agriculture and rice fields are reported in other studies (Yan et al., 2013; NGO et al., 2015).

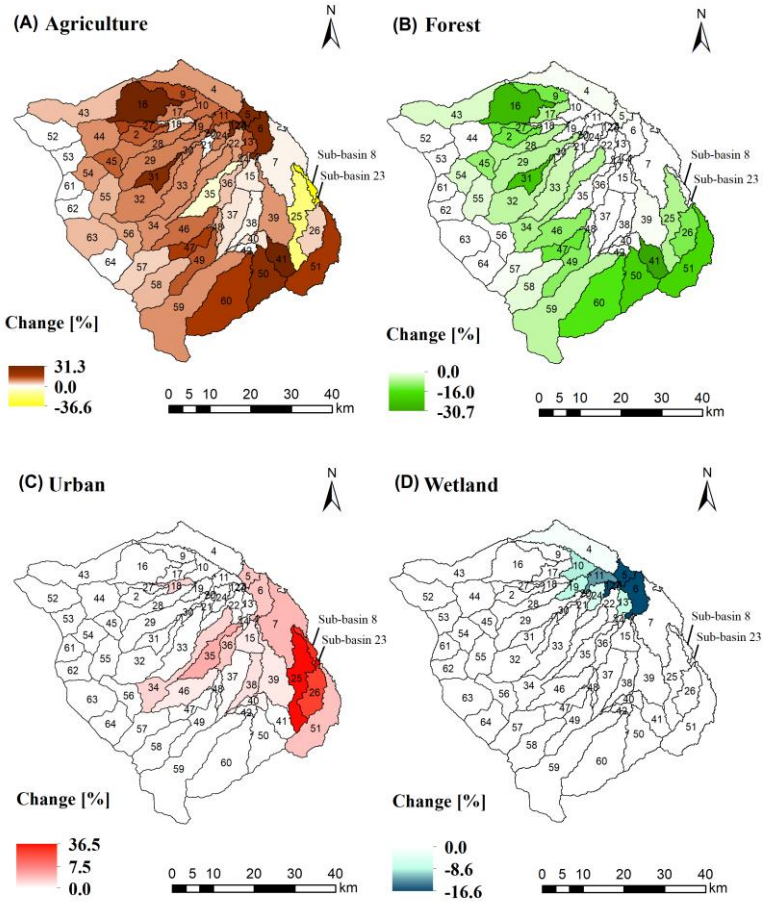

Fig. 2. Spatial distribution of land use changes at sub-basin level for (A) agriculture, (B) forest, (C) urban, and (D) wetland between 1990- 2013. Unchanged areas are shown in white.

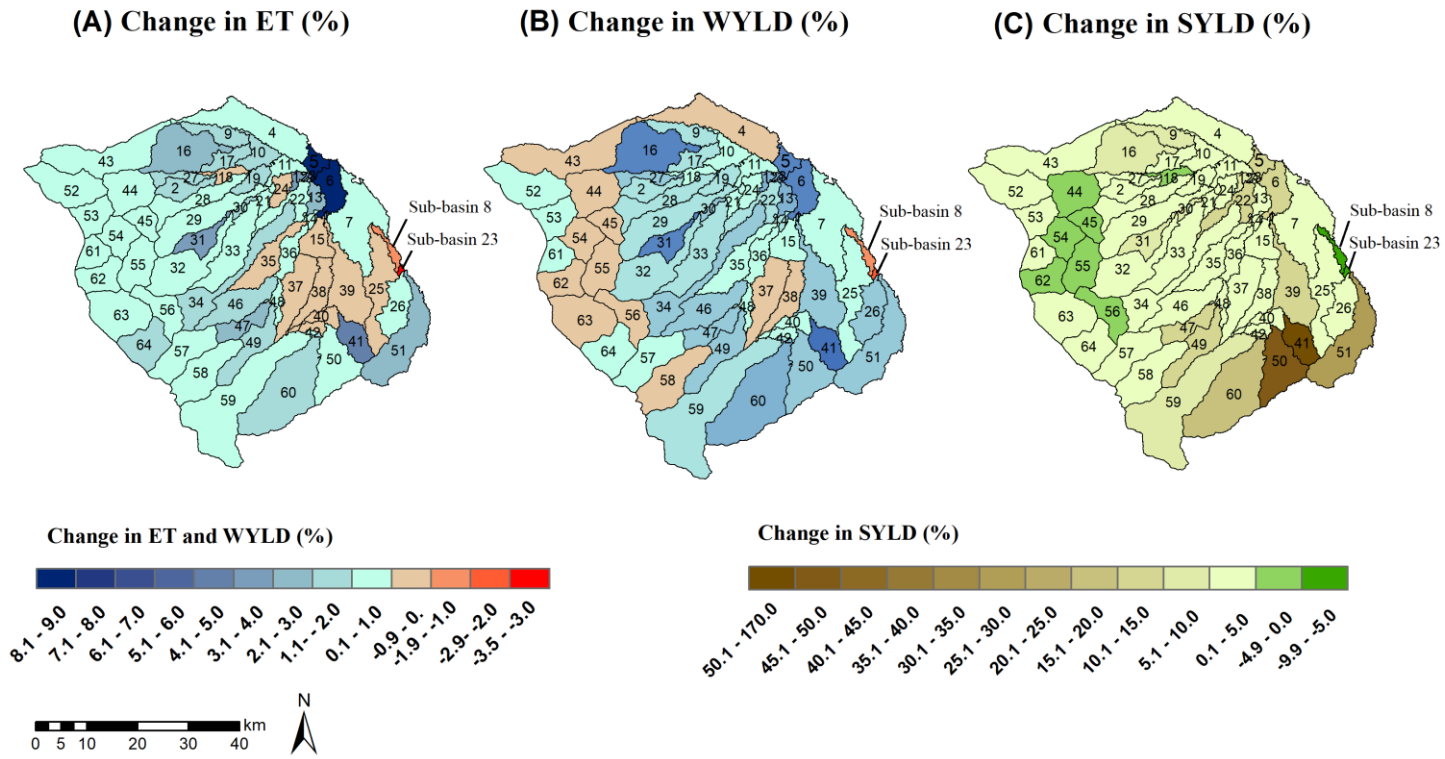

Fig. 3. Change in (A) ET, (B) WYLD, and (C) SYLD at the sub-basin level between 1990 and 2013.

3.3.3. Hydrological response at the seasonal time scale

The following analysis is focused on the monthly time scale impacts of land use change as more distinct differences in water balance components can be identified from the continuous land use changes. Seasonal responses to land use change have been identified in some other studies (e.g., Getachew and Melesse, 2012; Joorabian Shooshtari et al., 2017; Tigabu et al., 2019). Sub-basin 8 and sub-basin 16 are selected for further discussion as they are representative of the two main LULC transitions in the catchment: (i) from agriculture to urban (sub-basin 8) and (ii) from forest to agriculture (sub-basin 16). In sub-basin 8, the dominant land use change is an increase

of urban area (65% to 78%) at the expense of agriculture, whereas in sub-basin 16, the main land use change is an increase of agriculture area (52% to 77%) due to a decrease in forest. Fig. 4 shows the monthly hydrological response to the dynamic land use change in sub-basins 8 and 16. In both sub-basins, small differences are observed in the early years of the study period, while more pronounced seasonal patterns are generated with the increase of the magnitude of land use changes towards the end of the simulation period. In sub-basin 16, ET increases by up to 17.2 mm in dry season (April-August) and decreases by up to -2.7 mm in the wet season (September-February). The increase of ET is due to the increased irrigated agriculture (Schmidt et al., 2009). The decrease of ET shows the ability of forests to produce higher values of ET during the non-irrigated months than the agriculture. Guo et al. (2008) also found that the effects of increased forest area (at the expense of agricultural land) on ET and streamflow are particularly strong in the wet season.

In sub-basin 16, the expanded agriculture area resulted in an increase of WYLD by up to 17.6 mm in July 2012. The most significant changes of WYLD occur in the dry season as a consequence of the water withdrawal for the irrigation activities. The increased WYLD leads to a higher sedimentation rates during the irrigated months. The largest variation in SYLD is observed in October 2013 (+2.8 t/km^2). Kara et al. (2012) also reported a positive correlation between WYLD and SYLD for a small catchment located in eastern Alabama, USA (Kara et al., 2012).

In those sub-basins where the agriculture area increases at the expense of wetland area (e.g., sub-basins 3, 5, 6, 11, and 12) the observed seasonal patterns are similar to sub-basin 16 as agricultural land expansion cause more ET, WYLD, and SYLD simulation during the irrigation months, whereas less ET is simulated by the agriculture in the wet season than the wetland area.

In sub-basin 8, no discernible impacts on ET, WYLD, and SYLD are observed during 1990-2000 due to the small rate of urban expansion (less than 1%) between 1990-2000. In contrast, a significant land use change was noticed between 2000 and 2013, when the urban area expanded by more than 180%. Consequently, the maximum changes of ET, WYLD, and SYLD are associated with the maximum expansion of urban area. The monthly pattern of hydrological impacts in sub-basin 8 differs from the pattern in sub-basin 16 due to the different land use changes in the two sub-basins. In sub-basin 8, the most substantial decrease of ET occurs during the dry season months, with the maximum decrease in July and August. This decrease can mainly be attributed to a decrease of irrigation agriculture. In 2012, much more precipitation occurred in July (96 mm) in comparison with similar period in other years (e. g., 6, 7, 1 mm in July 2009, 2010, and 2011, respectively). Due to the heavy rains in the usually dry month, ET is less influenced by irrigation, which cause a smaller decrease in ET in 2012 (Fig. 4). ET increases by up to 3.14 mm with the largest variation in September 2012. This increase is due to the higher ET of urban area in the wet season in comparison with irrigation agriculture. Hence, the agricultural land use only increases the ET during the dry season due to increased consumption of irrigation water. Similar results about ET increase in the dry season due to the expansion of irrigated agriculture and ET reduction as a result of urban expansion were reported by Wagner et al. (2016). During the simulation period, a slight increase of WYLD can be observed in the rainy seasons (1.06 mm maximum in March 2012). A pronounced decrease of WYLD occurs in dry seasons, although, there is a slight increase of surface runoff. The highest difference of WYLD is -6.63 mm in July 2012. The main reason of decreased WYLD is the decrease in groundwater flow as a consequence of the increased impervious surface due to the urban expansion. Also, with the substitution of irrigated rice fields with urban areas reduction of WYLD could be

expected, as irrigation water does not add to WYLD anymore. In sub-basin 8, a similar pattern of WYLD responses were observed for the SYLD. The highest differences of SYDL is -7 t/km^2 in September 2011, where the WYLD is also decreased by -5.2 mm. However, no discernable changes were observed for the SYDL during the non-irrigated months, since no significant changes were observed for WYLD as well.

Similar results are presented in some other studies. For example, in a study conducted in the Bochung catchment in Korea**,** Kim et al. (2014) reported higher values of runoff for irrigated rice fields than urban area due to the low infiltration rate and Manning's coefficient. Wagner et al. (2013) reported only a slight increase of surface runoff as a consequence of an increase of built-up area at the beginning of the monsoon season in their study area. Moreover, as stated by Anand et al. (2018) the fraction of the surface runoff contribution from groundwater flow significantly decreased due to the development of urban area and decrease in cropland and forest area in the Ganga basin.

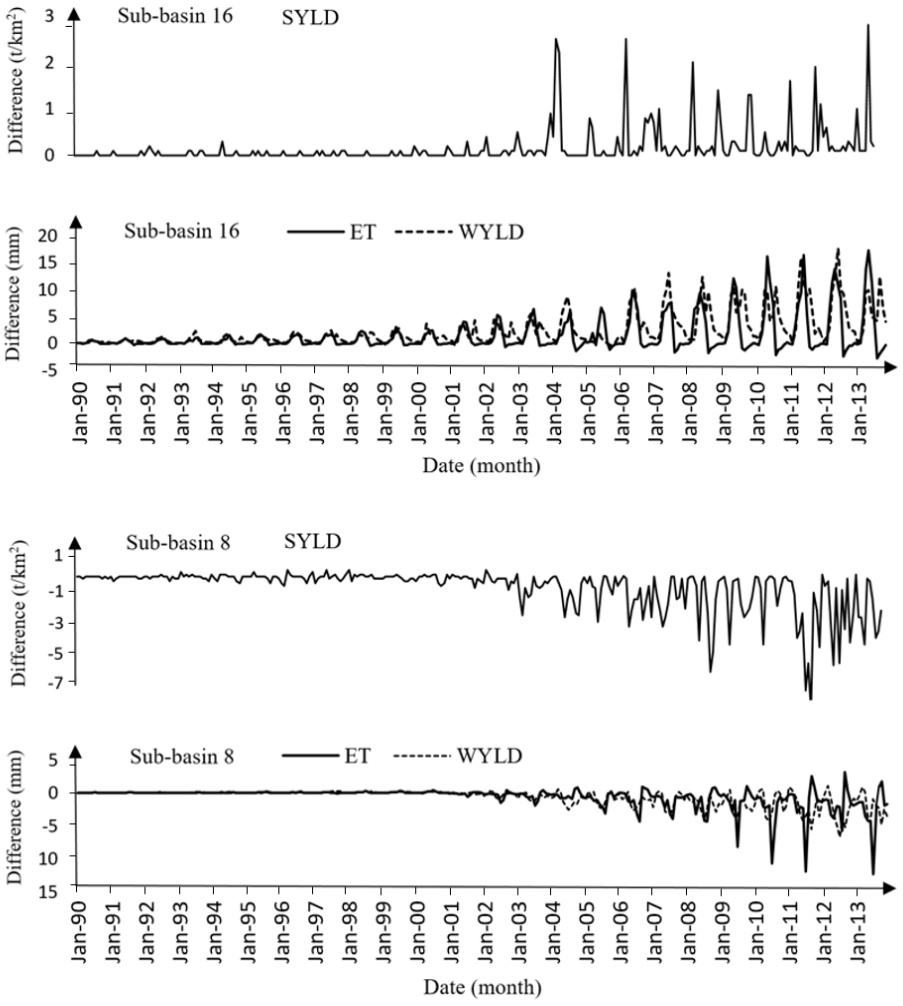

Fig. 4. Hydrologic impacts of dynamic land use changes in sub-basins 16 and 8 on the monthly time scale

4. Conclusion

This study demonstrates the importance of a dynamic assessment of land use change impacts on the hydrological response of a catchment. The major land use changes in the Anzali wetland catchment within the last 24 years are changes from forest to agricultural area (6.2%), which mainly occurred in the northwest to southeast of the catchment. As irrigation is applied to 70% of the agricultural area, it has a major impact on the hydrological response and soil loss of the

catchment. The hydrologic impacts were more pronounced on the seasonal time scale when compared to the annual time scale. The average annual evapotranspiration, water yield, and sedimentation increased due to the expansion of irrigation agriculture. This effect was partially balanced by urban sprawl in some areas of the catchment.

The increase in water yield causes more water discharge to the Anzali wetland during the dry seasons, which could disturb natural water regimes and wetting and drying patterns of the wetland. In addition, excessive sediment loads enter the wetland from upland agricultural erosion, which causes lower potential water storage and could negatively affect the ecological function and effective lifespan of the wetland. Moreover, the increased water consumption in dry season could result in an increase of water scarcity in the catchment. Large amounts of domestic and agricultural water demand are supplied by the irrigation canal which diverts water from Sefidrood river located outside of the catchment. Thus, the increased irrigated agriculture alongside with the ongoing urbanization will have more negative impacts on the natural flow and ecological environment of the Sefidrood river catchment due to the increased water demand. As it is likely that the rapid growth of the urban areas will progress (especially in Rasht city), it can be expected that the increased demand for food will probably increase the agriculture area at the expense of forest coverage in the lower elevations. Thus, an increased rate of forest lost might be another negative consequence of the urban expansion.

For the first time, hydrological modeling was conducted for the Anzali wetland catchment to assess the impacts of dynamic land use change on spatio-temporal changes in hydrological fluxes of the catchment. The findings from this study provide quantitative information that would help decision makers to implement effective land-use planning policies and water resource

management for a sustainable development of the catchment that considers interests of both wetlands and agriculture.

Acknowledgements

We gratefully acknowledge financial support from the Iranian National Science Foundation (INSF) and Iranian Water Resources Management Company.

References

Abbaspour, K.C., Yang, J., Maximov, I., Siber, R., Bogner, K., Mieleitner, J., Zobrist, J., 2007. Modeling hydrology and water quality in the pre-alpine/alpine Thur watershed using SWAT. J. Hydrol. 333, 413–430. https://doi.org/10.1016/j.jhydrol.2006.09.014.

Parajuli, P.B., 2019. Assessing model parameters sensitivity and uncertainty of streamflow, sediment, and nutrient transport using SWAT. Information Processing in Agriculture. 6(1), 61-72. https://doi.org/10.1016/j.inpa.2018.08.007.

Aladejana, O.O., Salami, A.T., Adetoro, O.-I.O., 2018. Hydrological responses to land degradation in the Northwest Benin Owena River Basin, Nigeria. J. Environ. Manag. 225, 300–312. https://doi.org/10.1016/j.jenvman.2018.07.095.

Ahiablame, L., Shakya, R., 2016. Modeling flood reduction effects of low impact development at a watershed scale. J. Environ. Manag. 171, 81–91. https://doi.org/10.1016/j.jenvman.2016.01.036.

Akbari, S., Loloi, A., Hemati, M.M., 2015. Gilan province statistical yearbook. Gilan Province Management and Planning Organization, Iran.

Allen, R.G., Jensen, M.E., Wright, J.L., Burman, R.D., 1989. Operational estimates of reference

evapotranspiration. Agron. J. 81, 650–662. http://dx.doi.org/10.2134/agronj1989.00021962008100040019x.

Arnold, J.G., Srinivasan, R.,Muttiah, R.S.,Williams, J.R., 1998. Large area hydrologicmodeling and assessment — part 1: model development. J. Am. Water Resour. Assoc. 34, 73–89. https://doi.org/10.1111/j.1752-1688.1998.tb05961.x.

Ashagrie, A. G., de Laat, P. J. M., de Wit, M. J. M., Tu, M., Uhlenbrook, S., 2006. Detecting the influence of land use changes on discharges and floods in the Meuse River Basin – the predictive power of a ninety-year rainfall-runoff relation? Hydrol. Earth Syst. Sci. 10, 691-701. https://doi.org/10.5194/hess-10-691-2006.

Ayivi, F., Jha. M.K., 2018. Estimation of water balance and water yield in the Reedy Fork-Buffalo Creek Watershed in North Carolina using SWAT. Int. Soil Water Conserv. Res. 203–213. https://doi.org/10.1016/j.iswcr.2018.03.007.

Bieger, K., Hörmann, G., Fohrer, N., 2012. Simulation of streamflow and sediment with the Soil Water Assessment Tool in a data scarce catchment in the Three Gorges Region. China. J. Environ. Qual. https://doi: 10.2134/jeq2011.0383.

Bieger, K., Hörmann, G., Fohrer, N., 2015. The impact of land use change in the Xiangxi Catchment (China) on water balance and sediment transport. Reg. Environ. Chang. 15, 485–498. http://dx.doi.org/10.1007/s10113-013-0429-3.

Biswas, S., Sudhakar, S., Desai, V. R., 2002. Remote Sensing and Geographic Information System Based Approach for Watershed Conservation. J. Surv Eng. 128(3), 108-124. https://doi.org/10.1061/(ASCE)0733-9453(2002)128:3(108).

Bormann, H., Elfert, S., 2010. Application of WaSiM-ETH model to Northern German lowland catchments: model performance in relation to catchment characteristics and sensitivity to land use change. Adv. Geosci. 27, 1–10. https://doi.org/10.5194/adgeo-27-1-2010, 2010.

Briak, H., Moussadek, R., Aboumaria, K., Mrabet, R., 2016. Assessing sediment yield in Kalaya gauged watershed (Northern Morocco) using GIS and SWAT model. Int. Soil Water Conserv. Res. 4, 177–185. https://doi.org/10.1016/j.iswcr.2016.08.002.

Burns, P., Nolin, A., 2014. Using atmospherically- corrected Landsat imagery to measure glacier area change in the cordillera Blanca, Peru from 1987 to 2010. Remote Sensing of Environment, 140, 165–178. https://doi.org/10.1016/j.rse.2013.08.026.

Chu, H-J., Lin, Y-P., Huang, C.W., Hsu, C-Y., Chen, H-Y., 2010. Modelling the hydrologic effects of dynamic land-use change using a distributed hydrologic model and a spatial land-use allocation model. Hydrol. Process. 24(18), 2538–2554. https://doi.org/10.1002/hyp.7667.

Cornelissen, T., Diekkrüger, B., Giertz, S., 2013. A comparison of hydrological models for assessing the impact of land use and climate change on discharge in a tropical catchment. J. Hydrol. 498:221–236. https://doi.org/10.1016/j.jhydrol.2013.06.016.

Crosta, A.P., Moore, J.M., 2007. Geological mapping using Landsat thematic mapper imagery in Almeria Province, South-east Spain. Int. J. Remote Sens, 10(3), 505-514. https://doi.org/10.1080/01431168908903888.

Douglas, I., 1983. The urban environment. Edward Arnold, London, Geotechnical Control Office, 1982. Mid-Levels Study: report on Geology, Hydrology and Soil Properties. Government Printer, Hong Kong.

Dwarakish, G.S., Ganasri, B.P., 2015. Impact of land use change on hydrological systems: A review of current modeling approaches. Cogent. Geoscience. 1, 1115691. http://dx.doi.org/10.1080/23312041.2015.1115691.

Elfert, S., Bormann, H., 2010. Simulated impact of past and possible future land use changes on the hydrological response of the Northern German lowland "Hunte" catchment. J. Hydrol. 383, 245–255. http://dx.doi.org/10.1016/j.jhydrol.2009.12.040.

FAO., 1995. Digital Soil Map of the World and Derived Soil Properties. Food and Agriculture Organization of the United Nations, Rome, Italy.

Fohrer, N., Haverkamp, S., Eckhardt, K., and Frede, H.-G., 2001. Hydrologic response to land use changes on the catchment scale, Phys. Chem. Earth Pt. B, 26, 577–582. https://doi.org/10.1016/S1464-1909(01)00052-1

Fontaine, T.A., T.S. Cruickshank, J.G. Arnold, and R.H. Hotchkiss. 2002. Development of a snowfall-snowmelt routine for mountainous terrain for the soil water assessment tool (SWAT). J. Hydrol. 262, 209–223. https://doi.org/10.1016/S0022-1694(02)00029-X.

Getachew, H.E., Melesse, A.M., 2012. The Impact of Land Use Change on the Hydrology of the Angereb Watershed, Ethiopia. Int. J. Cosmet. Sci. 1, 1-7. DOI: 10.5772/56266.

Ghaffari, G., Keesstra, S., Ghodousi, J., Ahmadi, H., 2010. SWAT-Simulated Hydrological Impact of Land-Use Change in the Zanjanrood Basin, Northwest Iran. Hydrol. Process. 24, 892–903. https://doi.org/10.1002/hyp.7530.

Ghafouri, M., Ghaderi, N., Tabatabaei, M., Versace, V., Ierodiaconou, D., Barry, D., Stagnitti, F. , 2010. Land use change and nutrients simulation for the Siah Darvishan basin of the Anzali

wetland region, Iran. Bull. Environ. Contam. Toxicol. 84, 240–244. https://doi.org/10.1007/s00128-009-9897-z.

Grey, O.P., Dale, F. St. G., Webber, D. F. St. G., Setegn, S.G., Melesse, A.M., 2014. Application of the Soil and Water Assessment Tool (SWAT Model) on a small tropical island (Great River Watershed, Jamaica) as a tool in Integrated Watershed and Coastal Zone Management. Int. J. Trop. Biol. 62 (Suppl. 3), 293-305. https://doi.org/10.15517/RBT.V62I0.15924.

Guo, H., Hu, Q., Jiang, T., 2008. Annual and seasonal streamflow responses to climate and land-cover changes in the Poyang Lake basin, China. J. Hydrol. 355, 106–122. https://doi.org/10.1016/j.jhydrol.2008.03.020.

Hwang, S.A., Hwang, S.J., Park, S.R., Lee, S.W., 2016. Examining the relationships between watershed urban land use and stream water quality using linear and generalized additive models. Water 8, 1–15. https://doi.org/10.3390/w8040155.

Im, S., Jang, C., Kim, C., Kim, H., 2009. Assessing the impacts of land use changes on watershed hydrology using MIKE SHE. Environ. Geol. 57, 231-239. https://doi.org/10.1007/s00254-008-1303-3.

Im, SJ., Park, SW., Jang, TI., 2007. Application of SCS curve number method for irrigated paddy field. KSCE J. Civ. Eng. 11, 51–56. https://doi.org/10.1007/BF02823372.

Jafari, M., Majedi, H., Monavari, S.M., Alesheikh, A.A., Kheirkhah Zarkesh, M., 2016. Dynamic simulation of urban expansion based on cellular automata and logistic regression model: Case study of the Hyrcanian Region of Iran. Sustainability, 8, 810. https://doi.org/10.3390/su8080810.

Jatin Anand, J., Gosain, A.K., Khosa, R., 2018. Prediction of land use changes based on Land Change Modeler and attribution of changes in the water balance of Ganga basin to land use

change using the SWAT model. Sci. Total Environ. 644, 503–519. https://doi.org/10.1016/j.scitotenv.2018.07.017.

Jing, Z., & Ross, M., 2015. Hydrologic modeling impacts of post-mining land use changes on streamflow of Peace River, Florida. Chin. Geogra. Sci. https://doi.org/10.1007/s11769-015-0745 2.

Joorabian Shooshtari, S., Shayesteh, K., Gholamalifard, M., 2017. Impacts of future land cover and climate change on the water balance in northern Iran. Hydrol. Sci. J. 62, 2655-2673. https://doi.org/10.1080/02626667.2017.1403028.

Kara, F., Loewenstein, E., Kalin, L., 2012. Changes in sediment and water yield downstream on a small watershed. Ekoloji. 21(84), 30–37. https://doi.org/10.5053/ekoloji.2012.844.

Kim, Y. J., Kim, H. D., and Jeon, J. H., 2014. Characteristics of Water Budget Components in Paddy Rice Field under the Asian Monsoon Climate: Application of HSPF-Paddy Model, Water. 6, 2041–2055. https://doi.org/10.3390/w6072041.

Koch, F.J., van Griensven, A., Uhlenbrook, S., Tekleab, S., Teferi, E., 2012. The effects of land use change on hydrological responses in the choke mountain range (Ethiopia) — a new approach addressing land use dynamics in the model SWAT. In: Seppelt, R., Voinov, A.A., Lange, S., Bankamp, D. (Eds.), International Environmental Modelling and Software Society (iEMSs) 2012 International Congress on Environmental Modelling and Software. Managing Resources of a Limited Planet: Pathways and Visions under Uncertainty. Sixth Biennial Meeting, Leipzig, Germany, pp. 3022–3029

Lamparter, G., Nobrega, R.L.B., Kovacs, K., Amorim, R.S., Gerold, G., 2016. Modelling hydrological impacts of agricultural expansion in two macro-catchments in Southern Amazonia, Brazil. Reg. Environ. Change. http://dx.doi.org/10.1007/s10113-016-1015-2

Legesse, D., Abiye, T. A., Vallet-Coulomb, C., Abate, H., 2010. Streamflow sensitivity to climate and land cover changes: Meki River, Ethiopia. Hydrol. Earth Syst. Sci. 14, 2277–2287. https://doi.org/10.5194/hess-14-2277-2010.

Li, P., Li, H., Yang, G., Zhang, Q., Diao, Y., 2018. Assessing the Hydrologic Impacts of Land Use Change in the Taihu Lake Basin of China from 1985 to 2010. Water. 10, 1512. https://doi.org/10.3390/w10111512.

Liang, X.Q., Wang, Z.B., Zhang, Y.X., Zhu, C.Y., Lin, L.M., Xu, L.X., 2016. No-tillage effects on N and P exports across a rice-planted watershed. Environ. Sci. Pollut. Re. 23, 8598–8609. https://doi.org/10.1007/s11356-016-6112-8.

Mao, D., Cherkauer, K. A., 2009. Impacts of land-use change on hydrologic responses in the Great Lakes region. Journal of Hydrology, 374, 71–82. https://doi.org/10.1016/j.jhydrol.2009.06.016.

Moriasi, D.N., Arnold, J.G., Van Liew, M.W., Binger, R.L., Harmel, R.D., Veith, T.L., 2007. Model evaluation guidelines for systematic quantification of accuracy in watershed simulations. Trans. ASABE. 50, 885–900.

Nash, J. E., Sutcliffe, J. V., 1992. River flow forecasting through conceptual models: Part I. A discussion of principles, J. Hydrol., 10, 282–290, 1970. https://doi.org/10.1016/0022-1694(92)90146-M.

National Resources Conservation Service (NRCS)., 2004. National Engineering Handbook, Part 630 Hydrology. USDA, Washington, DC.

Neitsch, S.L., Arnold, J.G., Kiniry, J.R., Srinivasan, R., Williams, J.R., 2010. Soil and Water Assessment Tool: Input/ Output File Documentation, Version 2009. Texas Water Resources Institute, Texas A&M University, College Station, Texas.

Ngo, T.S., Nguyen, D.B., Rajendra, P.S., 2015. Effect of land use change on runoff and sediment yield in Da River Basin of Hoa Binh province, Northwest Vietnam. J. Mt. Sci. 12, 1051–1064. http://dx.doi.org/10.1007/s11629-013-2925-9.

Nie, W., Yuan, Y., Kepner, W., Nash, M.S., Jackson, M., Erickson, C., 2011. Assessing impacts of land use and land cover changes on hydrology for the upper San Pedro watershed. J. Hydrol. 407, 105–114. https://doi.org/10.1016/j.jhydrol.2011.07.012.

Nitin Mishra, N., Kumar, S., 2015. Impact of Land Use Change on Groundwater Recharge in Haridwar District. 20th International Conference on Hydraulics, Water Resources and River Engineering, 17-19 December, India.

Pai, N., Saraswat, D., 2011. SWAT2009_LUC: A tool to activate the land use change module in SWAT 2009. Trans. ASABE, 54(5), 1649-1658. https://doi.org/10.13031/2013.39854.

Parsa Amini, V., Yavari, A., Nejadi, A., 2016. Spatio-temporal analysis of land use/land cover pattern changes in Arasbaran Biosphere Reserve: Iran. Model. Earth. Syst. Environ. https://doi.org/10.1007/s40808-016-0227-2.

Pinto Dias, L.C., Macedo, M.N., Costa, M.H., Coe, M.T., Neill, C., 2015. Effects of land cover change on evapotranspiration and streamflow of small catchments in the Upper Xingu River Basin, Central Brazil. Journal of Hydrology: Reg. Stud. 4, 108-122. https://doi.org/10.1016/j.ejrh.2015.05.010.

Plan and Budget Organization (PBO) of Iran., 2013. Report of Land Use Planning of the Gilan province.

Rogger, M., Alaoui, A., Bloeschl, G., 2017. Land use change impacts on floods at the catchment scale: Challenges and opportunities for future research, Water Resour. Res., 53, 5209–5219, https://doi.org/10.1002/2017WR020723.

Safeeq, M., Fares, A., 2012. Hydrologic response of a Hawaiian watershed to future climate change scenarios. Hydrol. Process. 26 (18), 2745–2764. http://dx.doi.org/10.1002/hyp.8328.

Sakaguchi, A., Eguchi, S., Kasuya, M., 2014. Examination of the water balance of irrigated paddy fields in SWAT 2009 using the curve number procedure and the pothole module. Soil. Sci. Plant. Nutr. 60(4), 551–564. https://doi.org/10.1080/00380768.2014.919834.

Schmidt, J., Kienzle, S. W., and Srinivasan, M. S., 2009. Estimating increased evapotranspiration losses caused by irrigated agriculture as part of the water balance of the Orari Catchment, Canterbury, New Zealand. J. Hydrol. (NZ), 48, 73–94. https://www.jstor.org/stable/43944979.

Shi, PJ., Yuan, Y., Zheng, J., Wang, J.A., Ge, Y., Qiu, G.Y., 2007. The effect of land use/cover change on surface runoff in Shenzhen region, China. https://doi.org/10.1016/j.catena.2006.04.015.

Shope, C.L., Maharjan, G.R., Tenhunen, J., Seo, B., Kim, K., Riley, J., Arnhold, S., Koellner, T., Ok, Y.S., Peiffer, S., 2014. Using the SWAT model to improve process descriptions and define hydrologic partitioning in South Korea. Hydrol. Earth Syst. Sci. 18, 539–557. https://doi.org/10.5194/hess-18-539-2014.

Soil Conservation Service, 1972, Section 4: Hydrology in National Engineering Handbook. SCS.

Stonestrom, D.A., Scanlon, B.R., Zhang, L., 2009. Introduction to special section on impacts of land use change on water resources. Water. Resour. Res. 45, 2–4. https://doi.org/ 10.1029/2009WR007937.

Teklay, A., Dile, Y.T., Setegn, S.G., Demissie, S.S., Asfaw, D.H., 2019. Evaluation of static and dynamic land use data for watershed hydrologic process simulation: A case study in Gummara watershed, Ethiopia. Catena. 172, 65–75. https://doi.org/10.1016/j.catena.2018.08.013.

Tigabu, T.B., Wagner, P.D., Hörmann, G., Fohrer, N., 2019. Modeling the impact of agricultural crops on the spatial and seasonal variability of water balance components in the Lake Tana Basin, Ethiopia. Hydrol. Res., accepted. https://doi.org/10.2166/nh.2019.170.

Tom, Lotz T., Opp, C., He, X., 2018. Factors of runoff generation in the Dongting Lake basin based on a SWAT model and implications of recent land cover change. Quat. Int. 475, 54-62. https://doi.org/10.1016/j.quaint.2017.03.057.

U.S. Geological Survey., 2019. Earth Explorer. Available at http://earthexplorer.usgs.gov.

Wagner, P.D., Bhallamudi, S.M., Narasimhan, B., Kantakumar, L.N., Sudheer, K.P., Kumar, S., Schneider, K., Fiener, P., 2016. Dynamic integration of land use changes in a hydrologic assessment of a rapidly developing Indian catchment. Sci. Total. Environ. 539, 153-164. http://dx.doi.org/10.1016/j.scitotenv.2015.08.148.

Wagner, P.D., Bhallamudi, S.M., Narasimhan, B., Kumar, S., Fohrer, N., Fiener, P., 2019. Comparing the effects of dynamic versus static representations of land use change in hydrologic impact assessments. Environ. Model. Softw. 122, 103987. https://doi.org/10.1016/j.envsoft.2017.06.023.

Wagner, P.D., Kumar, S., Schneider, K., 2013. An assessment of land use change impacts on the water resources of the Mula and Mutha Rivers catchment upstream of Pune, India. Hydrol. Earth Syst. Sci. 17, 2233–2246. http://dx.doi.org/10.5194/hess-17-2233-2013.

Wang, Q., Liu, R., Men, C., Guo, L., Miao, Y., 2018. Effect of dynamic land use inputs on improvement of SWAT model performance and uncertainty analysis of outputs. J. Hydrol. 563, 874-886. http://dx.doi.org/10.1016/j.jhydrol.2018.06.063.

Wang, G., Yang, H., Wang, L., Xu, Z., Xue, B., 2014. Using the SWAT model to assess impacts of land use changes on runoff generation in headwaters. Hydrol. Process. 28(3), 1032–1042.

https://doi.org/10.1002/hyp.9645.

Wilken, F., Wagner, P.D., Narasimhan, B., Fiener, P., 2017. Spatio-temporal patterns of land use and cropping frequency in a tropical catchment of South India. Appl. Geogr. 89, 124-132. https://doi.org/10.1016/j.apgeog.2017.10.011.

Williams, J. R., 1975. Sediment routing for agricultural watersheds, Water Resour. Bull. 11, 965–974. https://doi.org/10.1111/j.1752-1688.1975.tb01817.x.

Yan, B., Fang, N.F., Zhang, P.C., Shi, Z.H., 2013. Impacts of land use change on watershed streamflow and sediment yield: an assessment using hydrologic modelling and partial least squares regression. J. Hydrol. 484, 26–37. https://doi.org/10.1016/j.jhydrol.2013.01.008.

Yang, X., Lo, C.P., 2002. Using a time series of satellite imagery to detect land use and land cover changes in the Atlanta, Georgia metropolitan area Int. J. Remote Sens., 23 (9), 1775-1798. https://doi.org/10.1080/01431160110075802.

Zamani Hargalani, F., Karbassi, A., Monavari, S. M., 2014. A novel pollution index based on the bioavailability of elements: a study on Anzali wetland bed sediments. Environmental Monitoring and Assessment, 186(4), 2329–2348. https://doi.org/ 10.1007/s10661-013-3541-4

Zhang, Y.W., Shangguan, Z.P., 2016. The change of soil water storage in three land use types after 10 years on the Loess Plateau. Catena. 147, 87–95. http://doi.org/10.1016/j.catena.2016.06.036.

Zhao, A., Zhu, X., Liu, X., Pan, Y., Zuo, D., 2016. Impacts of land use change and climate variability on green and blue water resources in the Weihe river basin of northwest china. Catena. 137, 318–327. https://doi.org/10.1016/j.catena.2015.09.018.

Zhu, C., Li, Y., 2014. Long-term hydrological impacts of land use/land cover change from 1984 to 2010 in the Little River Watershed, Tenneesse. ISWCR. 2(2), 11-22. https://doi.org/10.1016/S2095-6339(15)30002-2.

Zubair, Younis., S.M, Ammar., A. 2018. Quantification of impact of changes in land use-land cover on hydrology in the upper Indus Basin, Pakistan. EJRS. 21, 255–263. https://doi.org/10.1016/j.ejrs.2017.11.001.

Declaration of interests

☒ The authors declare that they have no known competing financial interests or personal relationships that could have appeared to influence the work reported in this paper.

☐The authors declare the following financial interests/personal relationships which may be considered as potential competing interests:

Graphicala abstract

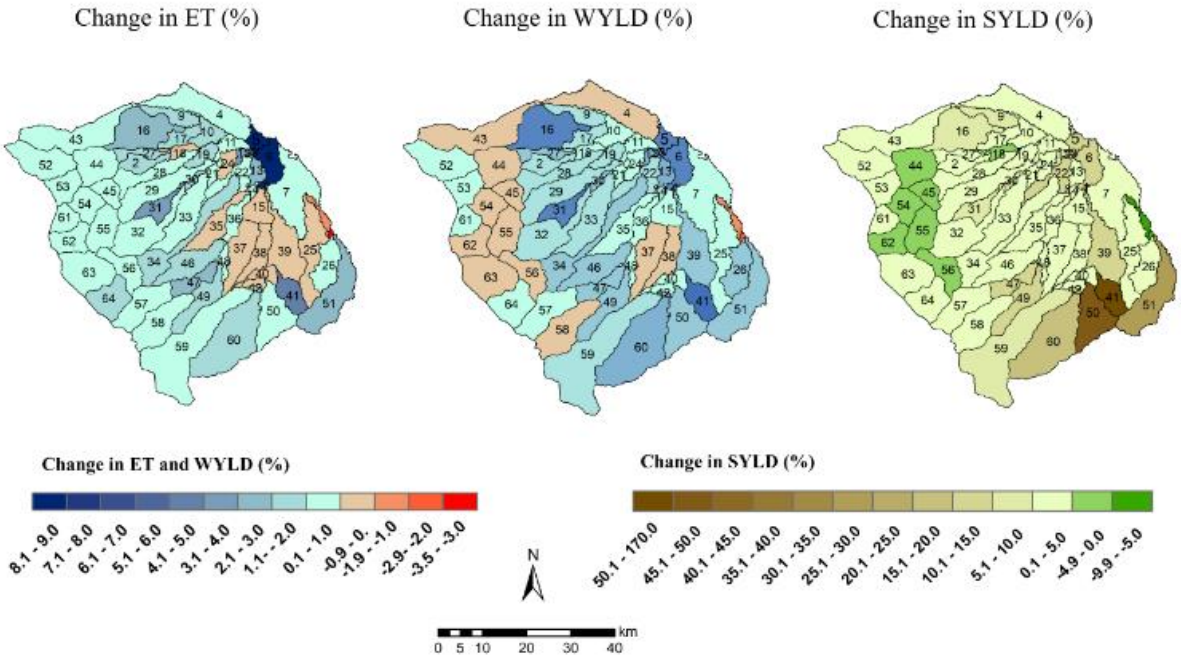

Highlights

- Effects of dynamic land use and land cover changes on hydrology were analyzed
- Main land use change between 1990 and 2013 was a change from forest to agriculture
- Increased sediment loads may affect the ecological function of the Anzali wetland